第31卷第5期 中 国 科 学 技 术 大 学 学 报 Vol. 31, No. 5
2001年10月 JOURNAL OF CHINA UNIVERSITY OF SCIENCE AND TECHNOLOGY Oct. 2001

Article ID: 0253-2778(2001)05-0518-10

Numerical Investigation on Two-dimensional Cylindrical Mud Impacting Walls and Mud Surfaces*

YUE Peng-tao[1], XU Sheng-li[1], LIU Da-you[2], DUAN Xin-ping[2]

(1. *Department of Mechanics and Mechanical Engineering, USTC, Hefei, Anhui* 230026)
(2. *Institute of Mechanics, Chinese Academy of Sciences, Beijing* 100080)

Abstract: Two-dimensional incompressible N-S equations for non-Newtonian fluid was solved by using MAC method in staggered grids. For mud, a numerical simulation was carried out of the impact of its cylinder on mud surface, and impact to walls from a broken dam. The results of water were also presented for comparison. The distortion of free surfaces is well simulated for mud and water. The evolution of free surfaces is in qualitative agreement with physical analysis. Because of the difference in constitutive relationship for water and mud, the evolutions of intruded surfaces are quite different when the cylinders impact the fluid surfaces. The free surface is more complicated for water, and impact load is also different for water and mud impacting the walls.

Key words: Non-Newtonian fluid, MAC method, incompressible flow, numerical simulation
CLC number: O24.82; O237 **Document code:** A

1 Introduction

Mudrock flow is one of the most severe natural disasters[1]. Because the problem is too complex, there is no perfect physical model to describe it at present. In fact, mud is the main component of mudrock flow, therefore, studies on mud flow will lead to a better understanding of the motion of mudrock flow[2]. Two questions remain unclear for studying mud flow. One is mud constitutive relationship, and the other is how to track mud free surfaces. Because mud compositions are different, mud constitutive relationships may be different. Generally, the constitutive relationships for most mud are similar to that of Bingham fluid. Therefore, in this paper, mud is treated as Bingham fluid.

Two kinds of methods are usually used to track the free surfaces. The first tracks the free surfaces

* **Received date:** 2000-09-11
Frundation item: The project was supported by National Nature Science Foundation of China (49771005)
Biography: YUE Pengtao, male, born in 1976, Ph.D candidate.

precisely, such as adaptive grids[3], mapping[4] etc. While the second tracks the free surfaces approximately, such as MAC[5] method and VOF[6] method. The MAC method was first used by Harlow and then Welch[5] extended it to solve three dimensional problems and in complex computational domains[7]. Yan[8] made a review on application of MAC method, and Tang[9] used it to study the bubble motion in non-Newtonian fluid. As for the VOF method, the volume fraction function F, satisfying the motion equation, is used to determine the position of free surfaces[6]. In summary, MAC and VOF methods are flexible in simulating problems on free surfaces with large distortion. But the boundary conditions can not be imposed accurately along the free surfaces because their positions are determined approximately.

It should be noted that only a few numerical works have been done on mud flow. In Ref. 2, the mapping method was used to study mud flow along a slope. Although the free surface can be determined accurately, the folding of free surfaces can not be well simulated. The purpose of this paper is to choose a suitable algorithm, and develop a general two-dimensional code to study the complicated mud flow along a slope, such as mud impacting the walls and fluid surfaces. The work involves (i) examining the code by a broken dam problem. (ii) conducting a numerical study on a mud cylinder impacting a mud surface, and mud impacting the walls from a broken dam. Also, the results for water were presented for comparison.

2 Governing Equations and Auxiliary Conditions

2.1 Physical model

The problem is shown in Fig. 1. Initially, mud column can be in any shape, but it is supposed to be cylindrical or rectangular for simplicity. MAC method was used to solve 2D unsteady N-S equations for incompressible non-Newtonian fluid. Pressure distribution was obtained by solving Poisson equation. Free surfaces were indicated by markers, which move at local fluid velocity. Mud possesses yield stress in its constitutive relationship, and is approximated by Bingham fluid in this paper. Its constitutive relationship can be expressed as:

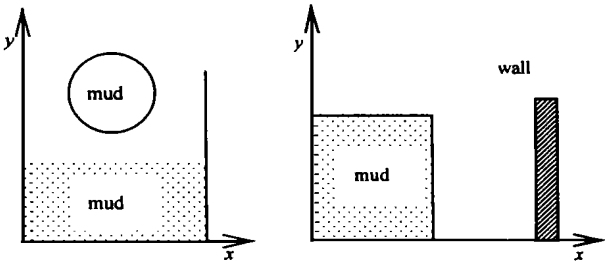

(a) Mud cylinder impacting mud surface

(b) Mud impacting walls

Fig. 1 Schematic of computational domain

$$\left.\begin{aligned} \tau_{ij} &= 2\mu_0\left(1+\frac{q_0}{q}\right)\cdot e_{ij} \quad (\tau_a > \tau_0) \\ e_{ij} &= 0 \qquad\qquad\qquad\quad (\tau_a \le \tau_0) \end{aligned}\right\}. \tag{1}$$

Where $q_0 = \tau_0/\mu_0$, τ_0 and μ_0 are yield stress and viscosity, respectively. τ_{ij} and e_{ij} are components of the stress and strain ratio tensors respectively. Equivalent strain ratio q and equivalent stress τ_a are expressed as:

$$q = [2u_x^2 + 2v_y^2 + (u_y + v_x)^2]^{1/2}, \tag{2}$$

$$\tau_a = [\frac{1}{2}\tau_{xx}^2 + \frac{1}{2}2\tau_{yy}^2 + \tau_{xy}^2]^{1/2}. \tag{3}$$

During the computation, it is convenient to rewrite eq. (1) as follows:

$$\tau_{ij} = 2\mu e_{ij} = 2\mu_0 f(q)\, e_{ij}, \tag{4}$$

where

$$f(q) = 1 + q_0/q. \tag{5}$$

Obviously, eq. (4) is singular at $q = 0$. But the following continuous function can approximate eq. (5).

$$f(q) = 1 + \frac{q_0 + Kq_0}{q_0 + Kq}\left[1 - \exp(-K(\frac{q_0 + Kq}{q_0 + Kq_0}))\right] \tag{6}$$

where K is a positive constant. The larger K is taken, the better approximation to Bingham fluid can be made. When K is zero, μ is reduced to constant μ_0, and the fluid is a Newtonian fluid.

1.2 Governing equations

By the constitutive relationship in eq. (4), the governing equations for 2D impressible fluid, including Newtonian and Non-Newtonian fluids, can be expressed as follows in Cartesian system:

$$\frac{\partial u}{\partial x} + \frac{\partial v}{\partial y} = 0, \tag{7}$$

$$\frac{\partial u}{\partial t} + \frac{\partial (uu)}{\partial x} + \frac{\partial (uv)}{\partial y} = \frac{1}{\rho_0}\left\{-\frac{\partial p}{\partial x} + \frac{\partial}{\partial x}(2\mu\frac{\partial u}{\partial x}) + \frac{\partial}{\partial y}\left[\mu(\frac{\partial u}{\partial y} + \frac{\partial v}{\partial x})\right]\right\} + g_x, \tag{8}$$

$$\frac{\partial v}{\partial t} + \frac{\partial (vu)}{\partial x} + \frac{\partial (vv)}{\partial y} = \frac{1}{\rho_0}\left\{-\frac{\partial p}{\partial y} + \frac{\partial}{\partial x}\left[\mu(\frac{\partial u}{\partial y} + \frac{\partial v}{\partial x})\right] + \frac{\partial}{\partial y}(2\mu\frac{\partial v}{\partial y})\right\} + g_y, \tag{9}$$

where ρ_0, p are density and pressure for mud, respectively. u, v and g_x, g_y are components of velocity $\vec{V}$ and gravity acceleration g_0 in x and y directions, respectively. g_0 and characteristic length L_0 are taken as reference parameters. Then, other reference parameters can be determined, such as velocity $(\sqrt{g_0 L_0})$, pressure $(\rho_0 g_0 L_0)$ and time $(\sqrt{L_0/g_0})$. Reynolds number is defined as $Re = \frac{\rho_0 g_0^{1/2} L_0^{3/2}}{\mu_0}$. Eqs. (7), (8) and (9) can be non-dimensionalized as follows:

$$\frac{\partial u}{\partial x} + \frac{\partial v}{\partial y} = 0, \tag{10}$$

$$\frac{\partial u}{\partial t} = \xi - \frac{\partial p}{\partial x}, \tag{11}$$

$$\frac{\partial v}{\partial t} = \eta - \frac{\partial p}{\partial y}, \tag{12}$$

where

$$\xi = -\left[\frac{\partial (uu)}{\partial x} + \frac{\partial (uv)}{\partial y}\right] + \frac{1}{Re}\left\{\frac{\partial}{\partial x}(2\mu\frac{\partial u}{\partial x}) + \frac{\partial}{\partial y}\left[\mu(\frac{\partial u}{\partial y} + \frac{\partial v}{\partial x})\right]\right\} + g_x \tag{13}$$

$$\eta = -\left[\frac{\partial (vu)}{\partial x} + \frac{\partial (vv)}{\partial y}\right] + \frac{1}{Re}\left\{\frac{\partial}{\partial x}\left[\mu(\frac{\partial u}{\partial y} + \frac{\partial v}{\partial x})\right] + \frac{\partial}{\partial y}(2\mu\frac{\partial v}{\partial y})\right\} + g_y \tag{14}$$

By differentiating eq. (11) with respect to x, and eq. (12) to y, a dimensionless Poisson equa-

tion for pressure can be derived as

$$\nabla^2 p = \frac{\partial \xi}{\partial x} + \frac{\partial \eta}{\partial y} + \frac{\partial}{\partial t}(\nabla \cdot \vec{V}). \tag{15}$$

Eqs. (10), (11) and (14) are to be solved in this paper. Continuity eq. (10) is a requirement in solving eq. (15).

1.3 Initial and boundary conditions

(i) Initial condition

As shown in Fig. 1, mud was supposed to be at rest initially, i.e. $\vec{V} = 0$.

(ii) Boundary conditions

As we know, the storage is very large for using MAC method. In this paper, the grid size is thicker than the boundary layer. Therefore, a free slip velocity was imposed ($\vec{V} \cdot \vec{n} = 0$) along the walls during the computation. The boundary condition for pressure was determined by eqs. (11) and (12).

(iii) Free surface conditions

In contrast to other stress, the surface tension and tangential stress can be neglected, but only atmosphere is considered along free surfaces. We get

in normal direction

$$\sigma_{ij} n_i n_j = - p_{\text{atm}}, \tag{16}$$

in tangential direction

$$\sigma_{ij} \tau_i n_j = 0. \tag{17}$$

Where $i, j = 1, 2$. $\vec{n} = (n_1, n_2)$, $\vec{\tau} = (\tau_1, \tau_2)$ are normal and tangential unit vectors along free surfaces respectively. p_{atm} is atmosphere.

2 Discretization of equations

Eqs. (11), (12) and (15) are discretized by MAC method in staggered grids. The definition of fluid variables are illustrated in Fig. 2, such as p, u, v and μ. In contrast to Newtonian fluid, the computation of viscosity μ is complicated, and dependent on local velocity. For mud fluid, it is noted that the forward difference is used for time derivative, and central difference is used for all spatial derivatives.

In order to reduce the accumulation of numerical errors, we let $\nabla \cdot \vec{V}^{n+1} = 0$ during the computation.

Simple average is used to get variables that are not defined at specified points. From the boundary conditions of free surfaces, velocity at the points out of boundaries or free surfaces can be obtained. For markers, their velocities are determined by area weighted average, and positions are updated by solving $\frac{\mathrm{d}x}{\mathrm{d}t} = u$ and $\frac{\mathrm{d}y}{\mathrm{d}t} = v$ by Euler's method.

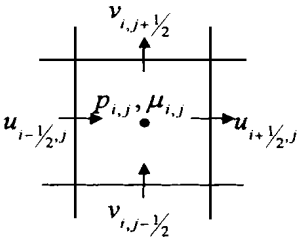

Fig. 2 Variables in cell

3 Results and discussion

3.1 Code validation

Before computations were conducted, the problem of a broken dam was chosen to validate the computer code. All conditions were the same as those in Ref. 5. Fluid is initially set to be a square of 1×1. Fig. 3 illustrates the distribution of free surfaces at different time intervals. In Fig. 3, water surface almost decreases one grid in the vertical direction at each time interval. In the horizontal direction, the wave front moves slowly at first, but evenly later on. A platform appears along the free surface, and increases its size with time passing. This resembles the pressure distribution at specified time for a shock tube problem. The wave front propagates right and rarefaction waves propagate left. The difference is that the water wave front is not so sharp as shock wave. A detailed comparison indicates that a good agreement is obtained between this paper and Ref. 5, including the free surface position and markers in each cell. In Ref 5, the computational results are also in good agreement with the experimental data. Thus, credibility of the computer code is indirectly validated in this paper.

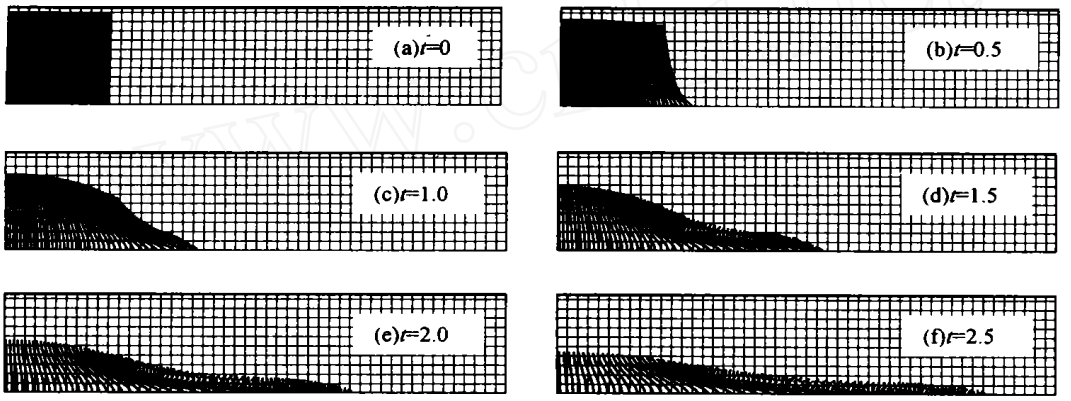

Fig. 3 Time history of water free surface for broken dam problems ($Re = 100$)

As Re increased, the free surfaces are almost the same as that in Fig. 3, but they become rougher. This can be attributed to (i) neglect of surface tension, which contributes to the stability of free surfaces; (ii) The viscous term becomes less dominated in governing equations. Similarly, fluid viscosity is helpful with the stability of free surfaces.

3.2 Mud cylinder impacting mud surface

Fig. 4 gives the distribution of free surfaces in the case of mud cylinder impacting mud surface. Initially, the cylinder center is located at $y = 1.5$ (Fig. 4(a)). If air drag is neglected, the cylinder remains unchanged during its falling because the normal stress equals atmosphere along the free surface. In Fig. 4(b), the cylinder has intruded into the mud surface. The intruded boundary can be seen clearly. A disturbance wave with very small amplitude, called the first wave, is generated at the intersected boundary and propagates outwards. In Fig. 4(c), the mud surface increases in height because the cylinder is immerged completely. A disturbance wave with large amplitude, called the second wave, is generated and propagates outwards. The intruded depth is increased further, but no funnel is

formed. In Fig. 4(d), the second wave impacts walls and leads the mud to climb along wall surfaces. The cylinder intrudes continuously, and a funnel is generated with a large opening. The intruded boundary is still very clear. The second wave reflects on the walls. The reflected disturbance wave, called the third wave, propagates to the center, and leads to fluid regression because of gravity effect. In Fig. 4(e), the third wave overlaps at the center, and a protuberance is formed. When time t increases from 3.0 to 6.0, the mud protuberance increases its height from 1.2 to 2.0. The intruded boundary is also distorted. After the protuberance arrives at its ceiling, it falls downwards by gravity. Finally, as shown in Fig. 4(f), mud surface vibrates, just like membrane vibration. No large disturbance waves are generated again. After a long time, the mud surface will slow down its vibration because of viscous dissipation.

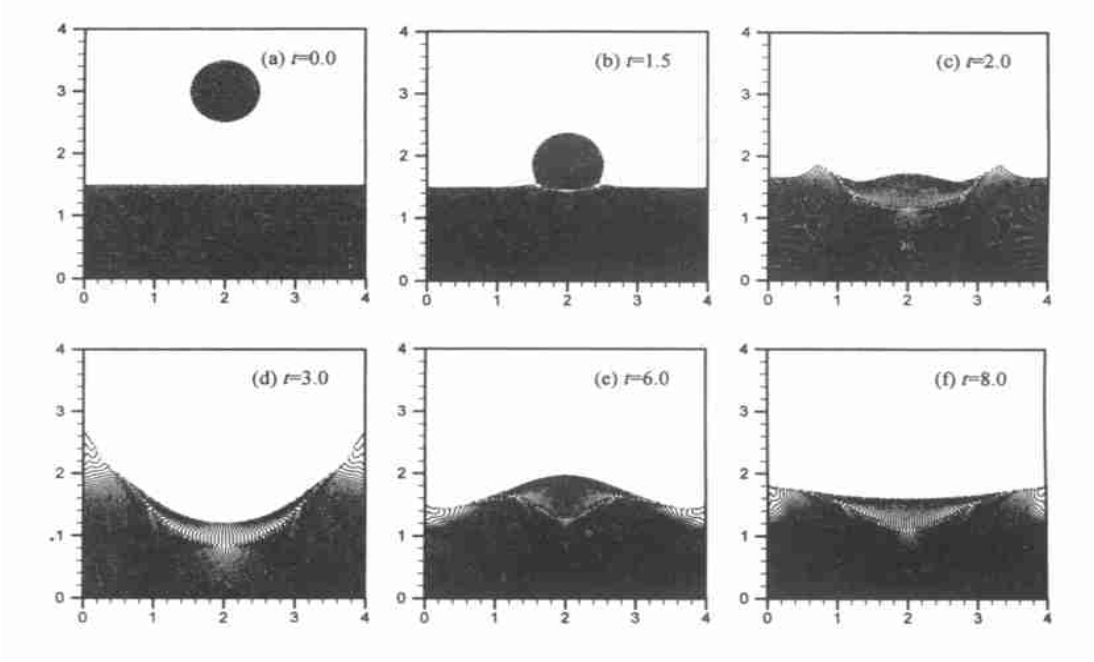

Fig. 4 Distribution of mud free surface (Re = 100, K = 20, q_0 = 20)

In contrast to Fig. 4, Fig. 5 presents the distribution of water free surfaces for comparison. Initially, the water cylinder is at the same position as mud (Fig. 4(a)). In Fig. 5(a), the water cylinder has impacted water surface. A disturbance wave, called the first wave is generated with small amplitude. The intruded surface can be observed clearly. In Fig. 5(b), the first wave impacts the walls, and leads two small clumps to climb along the walls (y = 1.8). The water surface increases its height because the cylinder is immerged completely in water. In the meantime, another disturbance wave, called the second wave, is generated with a large amplitude and a sharp corner on the water free surface. In Fig. 5(c), small water clumps arrive at y = 3 along the walls, and a funnel is formed with large opening and flat bottom. The intruded boundary is also very distinct. The second wave with folded free surface impacts the walls, and air is mixed into water. In Fig. 5(d), two small water clumps

arrive at $y = 3.6$, then, they begin to fall. Also, the second wave reflects on the walls. The third wave is formed and propagates to the center. Then, the depth and opening of the funnel are reduced. In Fig. 5(e), the two water clumps fall to $y = 1.8$ along the walls. The original intruded boundary becomes indistinct. The third wave overlaps at the center. A water protuberance is formed and arrives at $y = 3.2$. In Fig. 5(f), overlapped waves propagate outwards, and bubble flow is formed near the walls. The water surface stops its motion after a long period of time. In Ref. 10, the cylinder is initially tangential to the water surface, and the incident velocity is smaller than that in this paper. Therefore, the distortion of free surfaces is not so complex as that in this paper. In contrast to Fig. 4, the

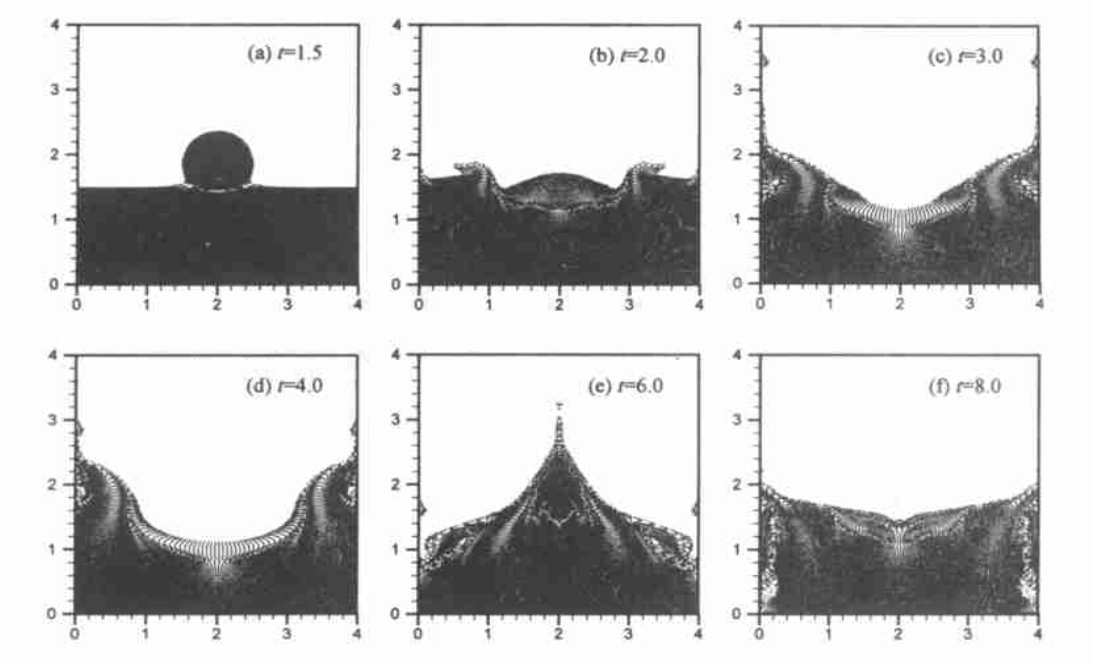

Fig. 5 Distribution of water free surface ($Re = 100$)

evolution of water free surfaces is quite different in Fig. 5. Although the mud free surface is not distorted seriously, the opening of the mud funnel is much larger. The reason is that the constitutive relationships are different for water and mud. The computed pressure and velocity distributions are omitted.

It is noted that there exists no obvious velocity shear layer near the intruded surface for mud and water cylinders impacting the fluid surfaces. The fluid will deform and even break up if it yields to the shear stress during the impacting.

3.3 Mud from broken dam impacting walls

Fig. 6 shows the evolution of mud free surfaces in the case of mud impacting walls. Before mud impacts the right wall, in Fig. 6(a)～6(c), it is just a broken dam problem of mud. In contrast to Fig. 3, the mud slows down because of large viscosity. Initially, mud stress is less than its yield stress at the right upper corner. So, the strain ratio is zero, and a sharp corner lasts for a long time. In Fig. 6(d)～6(e), a homogeneous mud layer is left on the horizon. After mud impacts the right wall, it

climbs along the right wall , and the ceiling height is very limited because of gravity and viscosity. In Fig. 6(e) ～6(f) , mud wave propagates to the left after mud collapses and impacts the mud layer.

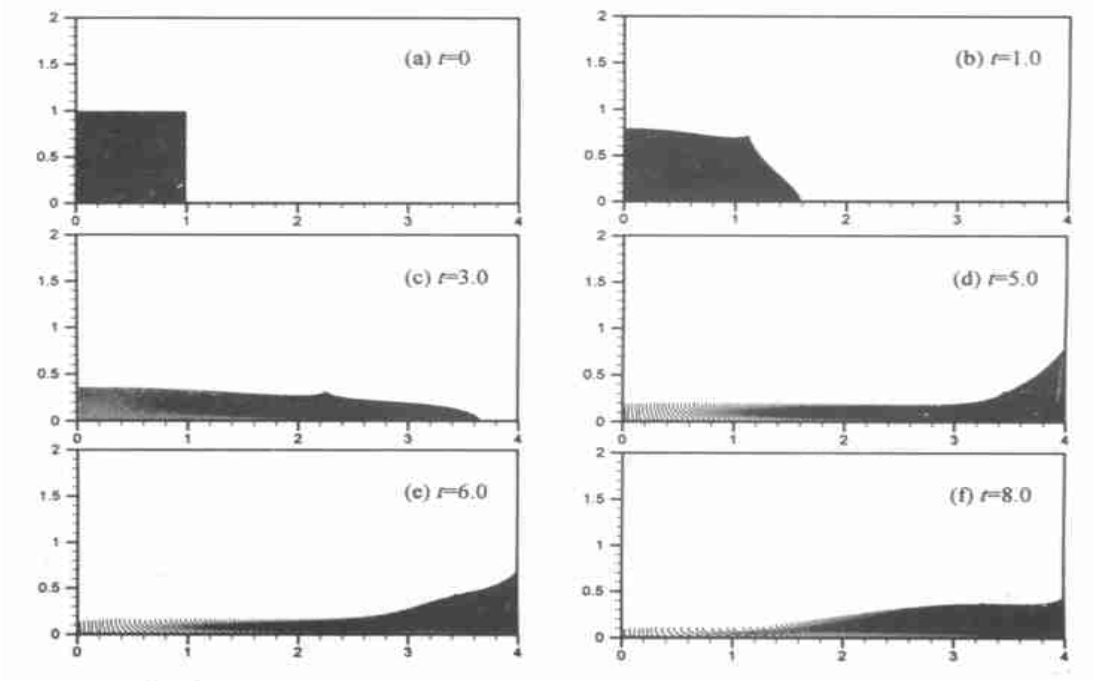

Fig. 6 Distribution of mud free surface (Re = 100 , K = 20 , q_0 = 20)

Fig. 7 presents the evolution of water free surfaces for comparison. In Fig. 7(a) , similar to mud , a homogeneous water layer is left on the horizon. Water climbs on the right wall. Because of gravity , water velocity is reduced to zero as water arrives at its ceiling height on the right wall. Then , it begins to fall. But water near the bottom of the wall still moves upwards. In Fig. 7(c) ～7(d) , the collapsing water impacts the water layer on the horizon , and the water free surface is folded. Then , a left moving water wave is formed. The free surface of the left propagating water wave becomes smooth in Fig. 7(e) ～7(f) , and impacts the left wall in Fig. 7(g) . Because the incident velocity is reduced considerably , the ceiling reached by water climbing on the left wall is lower than that on the right wall. After water collapses , a right-traveling water wave propagates on the water layer on the horizon , corresponding to a problem of broken dam on the water layer. In contrast to Fig. 3 , the front of the right-traveling water wave is sharp and a platform of water surface appears behind the wave front in Fig. 7 , similar to a shock wave in gas dynamics. When the right travelling water wave impacts the right wall again , the ceiling height is reduced even more. After a long time , water will stop its motion between the two walls.

For mud and water impacting the walls , the differences can be summarized as follows :

(1) When water and mud first impact the right wall , the mud layer is thicker than the water layer on the horizon.

(2) No large distorted free surface appears for mud impacting the walls.

(3) The ceiling height of mud climbing along the wall is lower than that of water.

(4) As shown in Fig. 8, mud arrives later at the right wall. Non-dimensional impact force F is

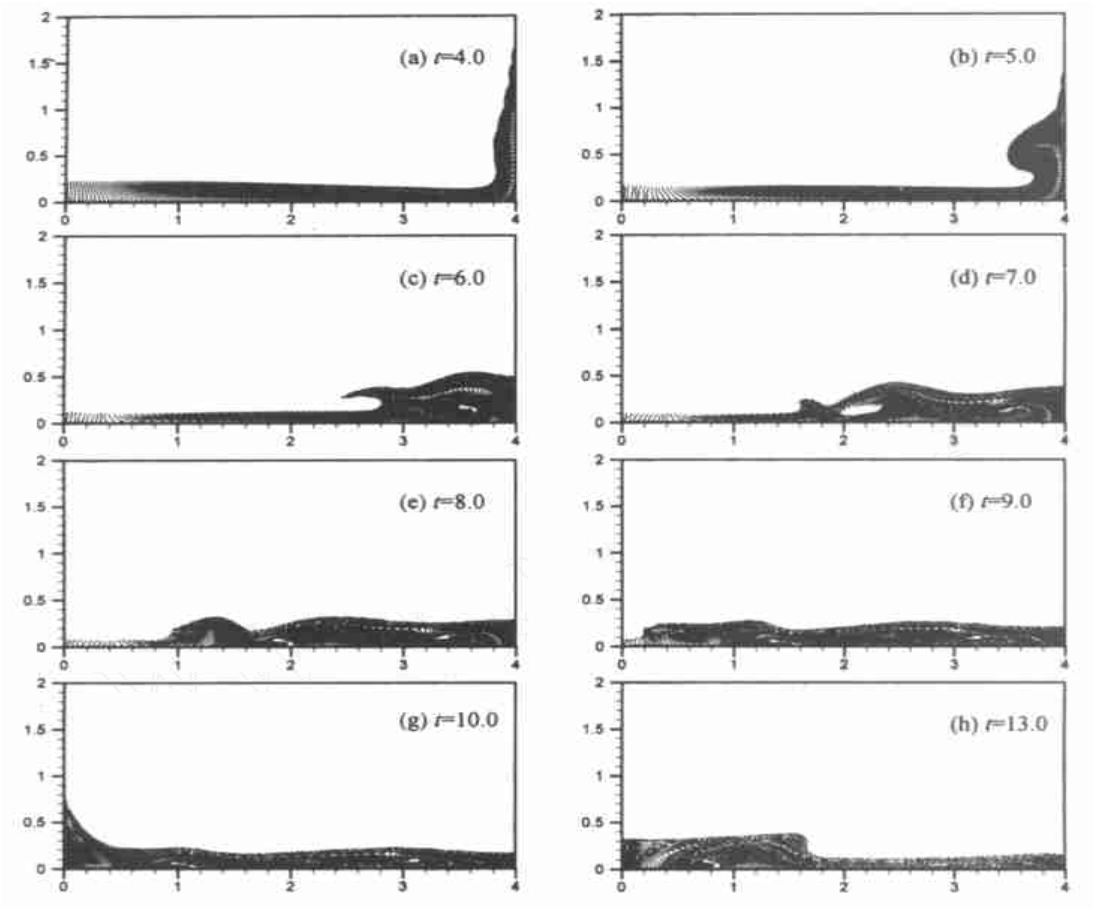

Fig. 7 Distribution of water free surface (Re = 100)

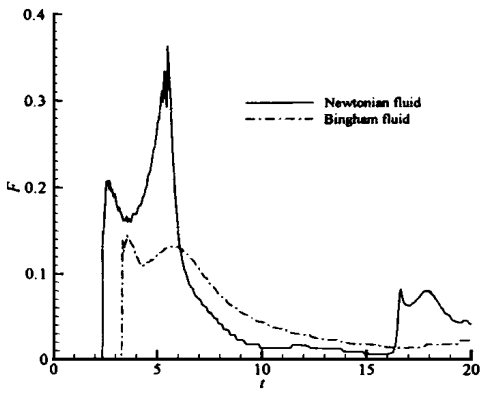

Fig. 8 Time history of impact load on the right wall

the integrated pressure at all grids along the right wall. The first impact force F for mud is less than that of water. There are two peaks for water in the first impact. The first peak denotes the impact load of fluid. The second peak includes the load when water collapses. Before t = 20, there are two impacts for water, but only one for mud.

4 Conclusion

(1) For Newtonian and non-Newtonian fluid impacting its surface and walls, the distortion and overlap of free surfaces can be well simulated by MAC method. The capability of MAC method is demonstrated further to deal with problems involvng complex free sur-

faces. The evolution of free surfaces is in qualitative agreement with theoretical analysis. The results provide a good foundation for studying the complicated flow further.

(2) Because of the difference in constitutive relationship, the evolution of free surfaces is different for mud and water. For mud, the folded free surface doesn't appear, but the funnel opening is larger when mud impacts its surface, and the impact load is smaller when it impacts the right wall.

By modifying the constitutive relationship, and auxiliary conditions, this code can be extended to study a variety of problems involving the free surfaces of Newtonian and non-Newtonian flow.

Reference

[1] LI Deji. Theory and application to prevent mudrock flow[M]. Beijing: Science press, 1997.

[2] Ma Fuhua. The numerical simulation of two dimensional unsteady mud flow with free surface [D]. Hefei: University of Science and Technology of China, 1999.

[3] Kang I S, Leal L G. Numerical solution of axisymmetric unsteady free-boundary problems at finite Reynolds number I. Finite difference scheme and its application to the deformation of a bubble in a unaxial straining flow[J]. Phys of Fluid, 1987, 30: 1 919～1 940.

[4] Dommermuth D G. The laminar interactions of a pair of vortex tubes with a free surface[J]. J Fluid Mech, 1993, 246: 91～115.

[5] Harlow F H, Welch J E. Numerical calculation of time-dependent viscous incompressible flow of fluid with free surface[J]. Phys of Fluid, 1965, 8 (13): 2 182～2 189.

[6] Hirt C W, Nichols B D. Volume of fluid (VOF) method for the dynamics of free boundaries[J]. J Computational Physics. 1981, 39: 201～225.

[7] Peyret R, Taylor T D. Computational methods for fluid flow [M]. New York: Springer-Verlag, 1983.

[8] Yan Kai. Development and application of MAC method[J]. Advances in Hydrodynamics, 1987, 2(3): 133～142 (in Chinese).

[9] Tang Yilong, Chen Yaosong, Chen Wenfang. Numerical simulation of bubble flow of non-Newtonian fluid[J]. Science in China, Series A, 23(7): 741～749 (in Chinese).

[10] Harlow F H, Shannon J P. Distortion of splashing liquid drop[J]. Science, 1967, 157: 547～550.

泥浆与液面、阻挡墙撞击的二维数值模拟

岳朋涛[1], 徐胜利[1], 刘大有[2], 段新平[2]

(1. 中国科学技术大学力学和机械工程系, 安徽合肥 230026; 2. 中国科学院力学研究所, 北京 100080)

摘要: 在交错网格中, 用 MAC 方法求解非牛顿流体的二维不可压 N-S 方程. 论文分别对圆柱形泥浆撞击液面、泥浆溃坝波撞击阻挡墙问题进行了数值模拟, 并与水的相应结果作了对照. 结果表明: 当与液面撞击时, 水和泥浆自由面随时间的演化图象与物理上的定性分析结果是一致的; 由于本构关系不同, 两者的侵彻自由面和液面运动均存在较大差异. 当水和泥浆与阻挡墙撞击时, 水的自由面变化要比泥浆复杂得多. 在相同的时间内, 左、右挡墙所受的冲击力和冲击次数也不相同.

关键词: 非牛顿流体; MAC 方法; 不可压流动; 数值模拟